

Efficacy of the Chinese Traditional Medicinal Herb *Celastrus orbiculatus* Thunb on Human Hepatocellular Carcinoma in an Orthotopic Fluorescent Nude Mouse Model

MAORONG WANG^{1,2*}, XIN ZHANG^{2*}, XI XIONG², ZHIGUO YANG², YU SUN³,
ZHIJIAN YANG³, ROBERT M. HOFFMAN^{4,5} and YANQING LIU^{1,6*}

¹The First Clinical College, Nanjing University of Chinese Medicine, Nanjing, P. R. China;

²Liver Disease Center and Department of Infectious Disease, Nanjing Jingdu Hospital, Nanjing, P. R. China;

³Origin Biosciences Inc., Nanjing, P. R. China;

⁴AntiCancer Inc., San Diego, CA, U.S.A.;

⁵Department of Surgery, University of California San Diego, San Diego, CA, U.S.A.;

⁶Institute of Chinese & Western Medicine, Yangzhou University, Yangzhou, P. R. China

Abstract. This study aimed to explore the inhibitory effect of *Celastrus orbiculatus* Thunb. (COT) on tumor growth, metastasis and angiogenesis of hepatocellular carcinoma (HCC) in an orthotopic nude mouse model using fluorescence imaging technology. Human HCC Hep-G2 cells expressing red fluorescent protein (RFP) were orthotopically implanted onto the liver of nude mice. One group of mice was treated with ethyl acetate extract of COT *p.o.* at a dose of 20 mg/kg starting on day 3 post-tumor implantation (early treatment). All other mice were randomized into four groups from day 20 post-tumor implantation and received either no treatment, oxaliplatin (25 mg/kg), or low-dose (20 mg/kg) or high-dose (40 mg/kg) COT. Real-time whole-body fluorescence imaging was performed to measure tumor growth and monitor metastasis development during the study. Vascular endothelial growth factor (VEGF) expression in the tumors collected at autopsy was analyzed by immunohistochemical staining and reverse transcription-polymerase chain reaction (RT-PCR). High-dose treatments, early treatment with COT, demonstrated significant efficacy on controlling tumor volume and tumor weight in the human HCC

Hep-G2 orthotopic tumor model. No significant differences were found for metastasis incidence among the different study groups. VEGF expression in the tumors was significantly reduced by oxaliplatin and COT treatment. This study demonstrates the inhibitory efficacy of COT on the growth of HCC tumor. VEGF inhibition may contribute in part to the inhibition of HCC tumor growth. The results of the present report suggest COT has potential to treat HCC.

Celastrus orbiculatus Thunb. (COT), a traditional Chinese medicinal herb, is widely distributed in native and its stem, root, leaves and fruit have been used for thousands of years as a remedy against cancer and inflammatory diseases (1). It has been reported that the extracts and some compounds isolated from COT have anti-tumor, anti-inflammatory, analgesic, antibacterial, antiviral, anti-fertility and other pharmacological activities (2). Previous experimental studies have shown that the ethyl acetate extract of COT has significant antitumor activity against various human tumor cell lines by inhibiting proliferation and inducing apoptosis in tumor cells (3, 4). A few *in vivo* studies have investigated the efficacy of COT on tumor growth and angiogenesis in animal tumor models (5-6). However, in the previous studies were either murine or subcutaneous tumor models, which demonstrate less relevance to the clinical situation than do orthotopic models (7). The present study used an orthotopic liver cancer model, with the tumor growing in its natural tissue microenvironment, enabling a clinical-like pattern of metastasis to occur (8). The tumor also expresses red fluorescent protein (RFP) facilitating *in vivo* visualization and quantification of tumor growth and metastasis development, and therefore, allows real-time evaluation of drugs on liver cancer without the need for any invasive procedure (9, 10).

*These Authors contributed equally to this study.

Correspondence to: Dr. Maorong Wang, Liver Disease Center and Department of Infectious Disease, Nanjing Jingdu Hospital, Nanjing, P. R. China, Tel: +86 2580864021, Fax: +86 2584546576, e-mail: maorongwang@126.com and Dr. Yanqing Liu, Institute of Chinese & Western Medicine, Yangzhou University, Yangzhou, P. R. China. E-mail: liuyq@yzu.edu.cn

Key Words: Traditional Chinese Medicinal herb, hepatocellular carcinoma, red fluorescent protein, orthotopic models, nude mice.

Materials and Methods

Animals. Fifty BALB/C male and female nu/nu nude mice, aged 4-6 weeks and weighing 20-25 g, were purchased from the Beijing Kelihua Laboratory Animal Center (Beijing, P. R. China). The mice were maintained in a HEPA-filtered environment at 24-25°C, with humidity of 50-60%. The animals were fed with autoclaved laboratory rodent diet. Animal experiments were approved by the Animal Committee of Nanjing Origin Biosciences, P. R. China.

Cell culture. The human hepatocellular carcinoma (HCC) cell line Hep-G2 was obtained from the Institute of Biochemistry and Cell Biology, Chinese Academy of Sciences (Shanghai, P. R. China). The cells were maintained in RPMI-1640 (GIBCO Life Technologies, New York, NY, USA) supplemented with 10% heat-inactivated fetal bovine serum (FBS; GIBCO) and cultured at 37°C in an incubator with 5% CO₂.

Retroviral RFP transduction of tumor cells. In order to obtain RFP-expressing Hep-G2 cells, the packaging PT67 cells transfected with a pDsRed-2 retrovirus vector were obtained from AntiCancer Inc. (San Diego, CA, USA). For RFP gene transduction, 25% confluent Hep-G2 cells were incubated with retroviral supernatants of the PT67 cells for 72 h. Fresh medium was replenished at this time. Cells were harvested by trypsin-EDTA 72 h after transduction and subcultured at a ratio of 1:15 into selective medium, which contained 400 µg/ml of G418. The level of G418 was increased to 800 µg/ml stepwise. Clones stably expressing RFP were isolated with cloning cylinders (Bel-Art Products, Pequannock, NJ, USA) with the use of trypsin-EDTA and were then amplified and transferred by conventional culture methods. High RFP-expressing clones of Hep-G-2 cells were then isolated in the absence of G418 for 10 passages to select for stable expression of RFP (11-13).

Surgical orthotopic implantation. Tumor stock of Hep-G2-RFP was established by subcutaneously injecting Hep-G2-RFP cells into the flank of nude mice. The tumor was maintained in nude mice subcutaneously as tumor stock prior to being used. On the day of implantation, the tumor was harvested from the subcutaneous site and placed in RPMI-1640 medium. Strong RFP expression of the Hep-G2-RFP tumor tissue was confirmed by fluorescence microscopy (see below). Necrotic tissues were removed and viable tissues were then cut into 1 mm³ pieces. Test animals were transplanted by surgical orthotopic implantation (SOI) using tumor tissue fragments harvested from stock tumors. The animals were anesthetized by injection of 0.02 ml of solution of 50% ketamine, 38% xylazine, and 12% acepromazine maleate. The surgical area was sterilized using iodine solution and alcohol. An incision of approximately 1 cm long was made in the upper abdomen of the nude mouse using surgical scissors. The liver was exposed and one fragment of tumor tissue was sutured to the left lobe with sterile 8-0 surgical sutures (nylon; Ethicon Inc., NJ, USA). The abdomen was closed with sterile 6-0 surgical sutures (silk; Ethicon Inc.). All surgical procedures and animal manipulations were conducted under HEPA-filtered laminar-flow hoods with the aid of a ×7 microscope (Olympus).

Antitumor treatment. The ethyl acetate extract of COT used in the study was supplied by the Nanjing University of Chinese Medicine and kept at 4°C until use. COT was dissolved with Dimethyl

Sulfoxide (final concentration below 0.05% by volume) and diluted with saline before administration. Mice implanted with Hep-G2-RFP were monitored for tumor growth by non-invasive fluorescence imaging (see below) after tumor implantation. Ten mice were randomly selected for early treatment (group 5) and were treated with COT *via* oral gavage at a dose of 20 mg/kg starting from day 3 post-tumor implantation. All other mice were randomized into four groups of 10 mice each after tumor growth was confirmed by fluorescence imaging. Group 1 served as the negative control and did not receive any treatment. Group 2 received oxaliplatin treatment *via* tail vein at a dose of 25 mg/kg. Groups 3 and 4 were treated with COT *via* oral gavage at 20 and 40 mg/kg/dose, respectively. Dosing for both COT and oxaliplatin was performed daily until the end of the study. Each animal was examined at least once a day from initiation of treatment for clinical signs during the treatment and observation period. The body weight for each animal was measured twice a week to monitor for toxicity of COT.

Tumor measurement by fluorescence imaging. During the study, the animals were monitored for tumor growth and metastasis by whole-body fluorescence imaging. Tumor area was calculated using the formula $(L \times W^2) \times 0.5$, where W and L represent the minor and major perpendicular dimensions, respectively. At the end of the study, all mice were sacrificed and open fluorescent imaging was performed. Primary tumors and all metastases to distant organs, including the mesentery lymph nodes, lung, liver, abdominal cavity and thoracic cavity, were carefully imaged. After performing fluorescence imaging, the primary tumor was removed from each mouse and weighed. A fluorescence stereo microscope (model MZ650; Nanjing Optic Instrument Inc., P. R. China) equipped with D510 long-pass and HQ600/50 band-pass emission filters (Chroma Technology, Brattleboro, VT, USA) and a cooled color charge-coupled device camera (Qimaging, BC, Canada) was used. Selective excitation of RFP was produced through an illuminator equipped with HQ470/40 and HQ540/40 excitation band-pass filters (Chroma Technology). Images were processed and analyzed with the use of image-pro plus 6.0 software (Media Cybernetics, Silver Spring, MD, USA).

Histological and immunohistochemical analysis. At autopsy, the tissues from the primary tumors and any organs with metastases were harvested. Histopathology was performed using standard H&E staining methods. Vascular endothelial growth factor (VEGF) expression was determined by immunohistochemical staining with antibody against VEGF using VEGF S-P kit (Sangon Biotech, Shanghai, P. R. China) according to the manufacturer's instructions. Briefly, paraffin-embedded, formalin-fixed tissue sections of 5 µm were mounted on microscope slides. Tissue sections were then dried overnight at 60°C, dewaxed in xylene and rehydrated with distilled water. Endogenous peroxidase was inhibited by 1% H₂O₂ in methanol for 10 min. Incubation with the anti-VEGF antibody (1:400) was performed overnight at room temperature followed by incubation with secondary antibody and streptavidin-avidin-biotin. The peroxidase reaction was performed using 3,3'-diaminobenzidine tetrahydrochloride (DAB). Finally, sections were counterstained with Harris hematoxylin and were examined under a microscope.

Immunoreactivity for VEGF was scored when the cytoplasm of the cancer cells stained brown. To quantitate the immunohistochemically determined expression of VEGF, the images from the

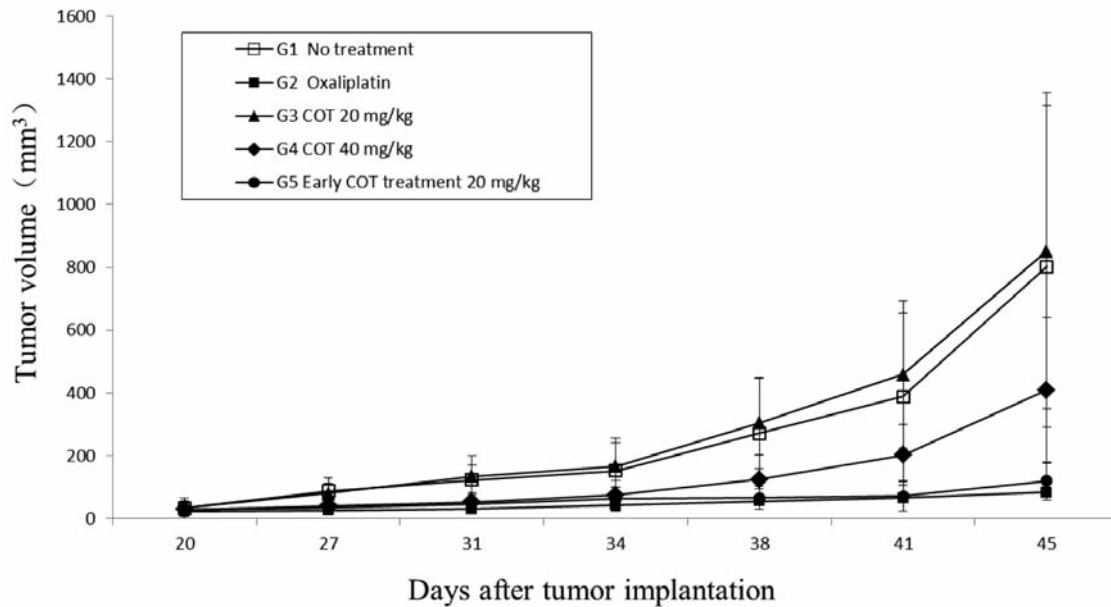


Figure 1. Efficacy of *Celstrus orbiculatus* Thunb (*COT*) and oxaliplatin on tumor growth in the orthotopic human Hep-G2- red fluorescent protein (*RFP*) hepatocellular carcinoma (*HCC*) nude mouse model. Tumor growth was monitored and quantified by real-time whole-body fluorescence imaging. At day 45 after treatment, Tumor volumes were significantly reduced in mice treated with high-dose (40 mg/kg) *COT* ($410.0 \pm 231.6 \text{ mm}^3$) and early treatment with *COT* (20 mg/kg) ($120.5 \pm 60.1 \text{ mm}^3$) and oxaliplatin ($83.8 \pm 23.5 \text{ mm}^3$) compared to the control group ($803.1 \pm 512.3 \text{ mm}^3$) ($p < 0.05$).

sections with positive VEGF expression were captured under the same conditions and analyzed using image-pro plus 6.0 (IPP) software (Media Cybernetics, Silver Spring, Maryland, USA). Average optical density of the entire field of view (D) was calculated using the formula: $D = \text{IOD sum} / \text{area sum}$, where IOD sum and area sum are integrated optical density and area in the entire field of view, respectively.

Reverse transcription-polymerase chain reaction (RT-PCR) analysis. RT-PCR was used to analyze the expression of *VEGF* and glyceraldehyde-3-phosphate dehydrogenase (*GAPDH*) mRNAs. Total RNA extraction and purification were performed with an RNA extraction kit (Promega, Madison, Wisconsin, USA) according to the manufacturer's instructions. The *VEGF* primers were synthesized by Sangon Biological Engineering and Technology Services (Shanghai, P. R. China). The sequence of the *VEGF* sense primer used was 5'-GGGGATCCGCTCCGAAACCATG AACTT-3', the antisense primer used was 5'-CCC GAATC TCCTGGTGAGAGATCTGGTT-3' and the amplification length was 550 bp. RT-PCR was performed with an Access RT-PCR kit (Promega) according to the manufacturer's instructions. Each reaction mixture contained 10 μl 5 \times AMV/Tfl reaction buffer, 1 μl dNTP mix, 1 μl Tfl DNA polymerase, 1 μl AMV reverse transcriptase, 3 μl 25 mmol/l magnesium sulfate, 0.5 μg total RNA, and 50 pmol of each *VEGF* and *GAPDH* primers. Reaction conditions were: 48°C for 45 min for reverse transcription, 94°C incubation for 2 min to denature hybridized RNA/cDNA and inactive AMV reverse transcriptase. Reaction conditions for amplification of target gene were: 40 cycles of denaturing at 94°C for 30 s, annealing at 55°C for 30 s, extension at 68°C for 90 s and final extension at 68°C for 7 min. PCR products were analyzed on

2% agarose gels and stained with ethidium bromide. Gels were scanned and images were analyzed using UN-SCAN-IT software (Silk Scientific, Orem, UT, USA), and the VEGF/*GAPDH* ratio was calculated.

Statistical analysis. The *t*-test with an α equal to 0.05 (two-sided) was used to measure differences in tumor volumes, final tumor weights and body weights among the various groups. Fisher's exact test was used to compare metastatic incidence to the LNs and distant organs between the treated and untreated groups. A *p*-value less than 0.05 was considered to be statistically significant.

Results

Effect of *COT* and Oxaliplatin on primary tumor growth. *COT* early treatment resulted in significantly smaller tumors compared to untreated control during the course of treatment ($p < 0.01$) (Figures 1 and 2A). In the late-treatment groups, the tumor size was significantly reduced by high-dose (40 mg/kg) *COT* compared to the control group at 11 and 18 days after treatment initiation ($p < 0.01$), although no significant difference was obtained at day 25 after treatment ($p > 0.05$). Low-dose *COT* (20 mg/kg) treatment was not inhibitory on primary tumor growth ($p > 0.05$). Significant tumor size reduction was observed with oxaliplatin treatment compared to the control at all time points in the course of treatment ($p < 0.01$). There was no significant difference for tumor size reduction between early *COT* treatment and oxaliplatin treatment.

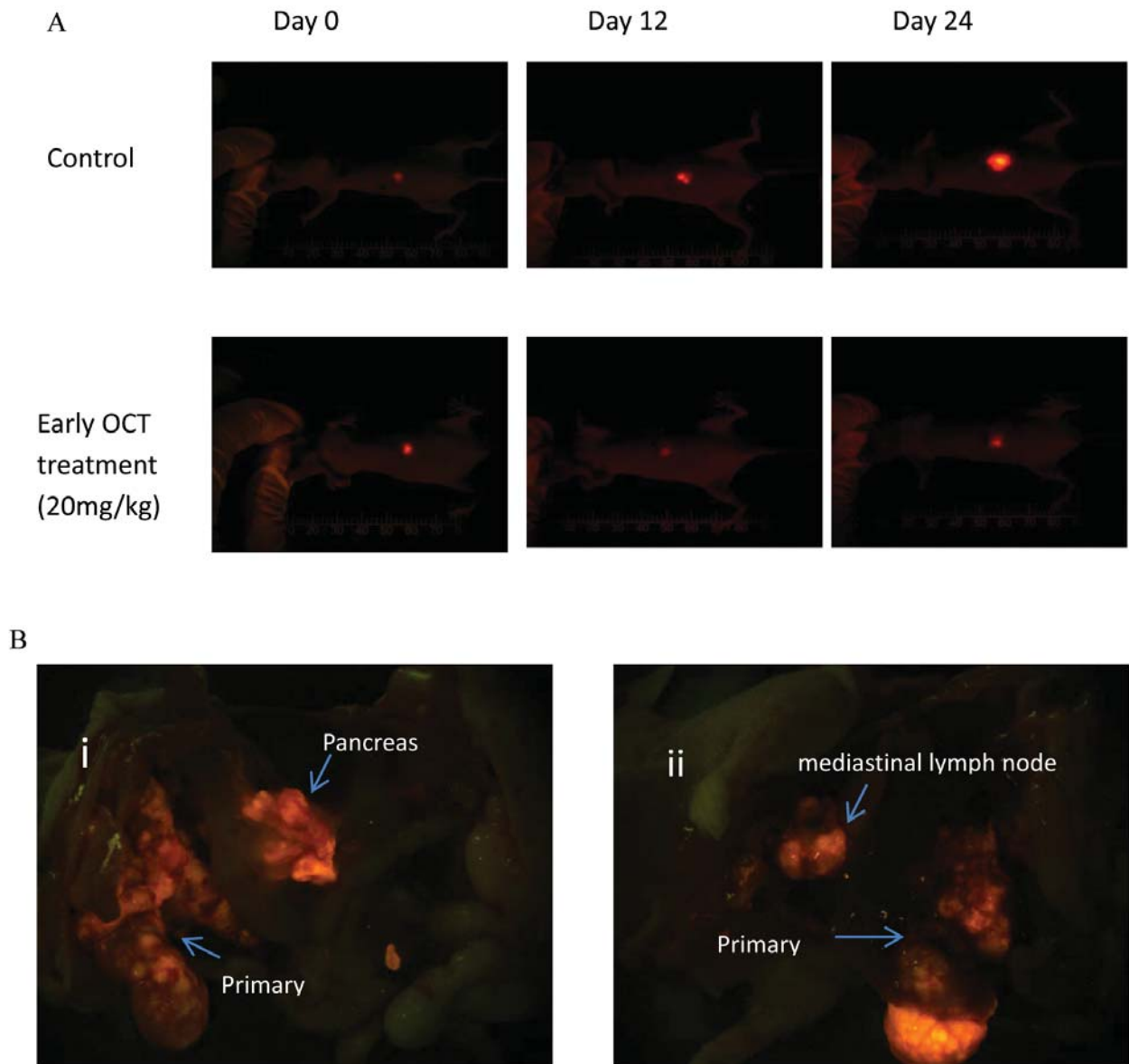


Figure 2. A: Sequential *in vivo* whole-body fluorescence imaging of tumor progression over time in the mice treated with *Celastrus orbiculatus* Thunb (COT) and oxaliplatin in the orthotopic human Hep-G2- red fluorescent protein (RFP) hepatocellular carcinoma(HCC) nude mouse model. Panels depict a representative mouse from each of early COT treatment and control group on days 0, 12, and 24 after treatment initiation. B: Open fluorescence imaging of mice at autopsy. The images display metastases in the pancreas (i) and mediastinal lymph node (ii) in the untreated orthotopic Hep-G2-RFP HCC mouse model.

At the end of the study, tumors were dissected and tumor weights were determined for each animal. The mean tumor weights for each group are presented in Figure 3. Tumor weights were significantly reduced compared to the control by early COT treatment, late treatment with high-dose COT and oxaliplatin treatment ($p < 0.05$). No significant tumor weight reduction was found by low-dose COT treatment compared to the control group ($p > 0.05$).

Efficacy of COT and oxaliplatin on metastasis. Fluorescence whole-body imaging was used to monitor metastasis during the study. All animals were opened at sacrifice. Fluorescence open imaging was performed to locate RFP-expressing metastases. Potential metastasis to local and distant organs including the lymph nodes, spleen, lung, liver, diaphragm, abdominal cavity, and thoracic cavity was carefully explored (Figure 2B). No significant

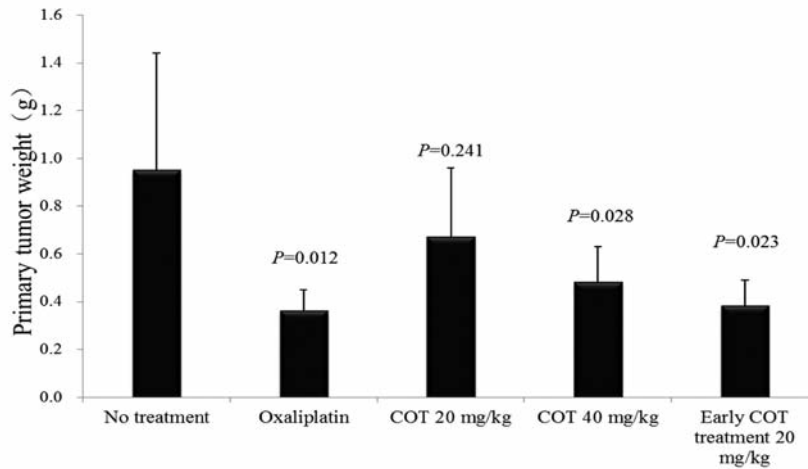


Figure 3. Efficacy of *Celastus orbiculatus* Thunb (COT) and oxaliplatin on tumor weights in the orthotopic human Hep-G2- red fluorescent protein (RFP) hepatocellular carcinoma(HCC) nude mouse model. Primary tumors were excised and tumor weights were determined for each animal at autopsy. Tumor weights were significantly reduced compared to the control (0.95g±0.49g) by early COT treatment (0.38g±0.11g, $p=0.023$), high-dose COT (0.48g±0.15g, $p=0.028$) and oxaliplatin (0.36g±0.09g, $p=0.012$) treatments.

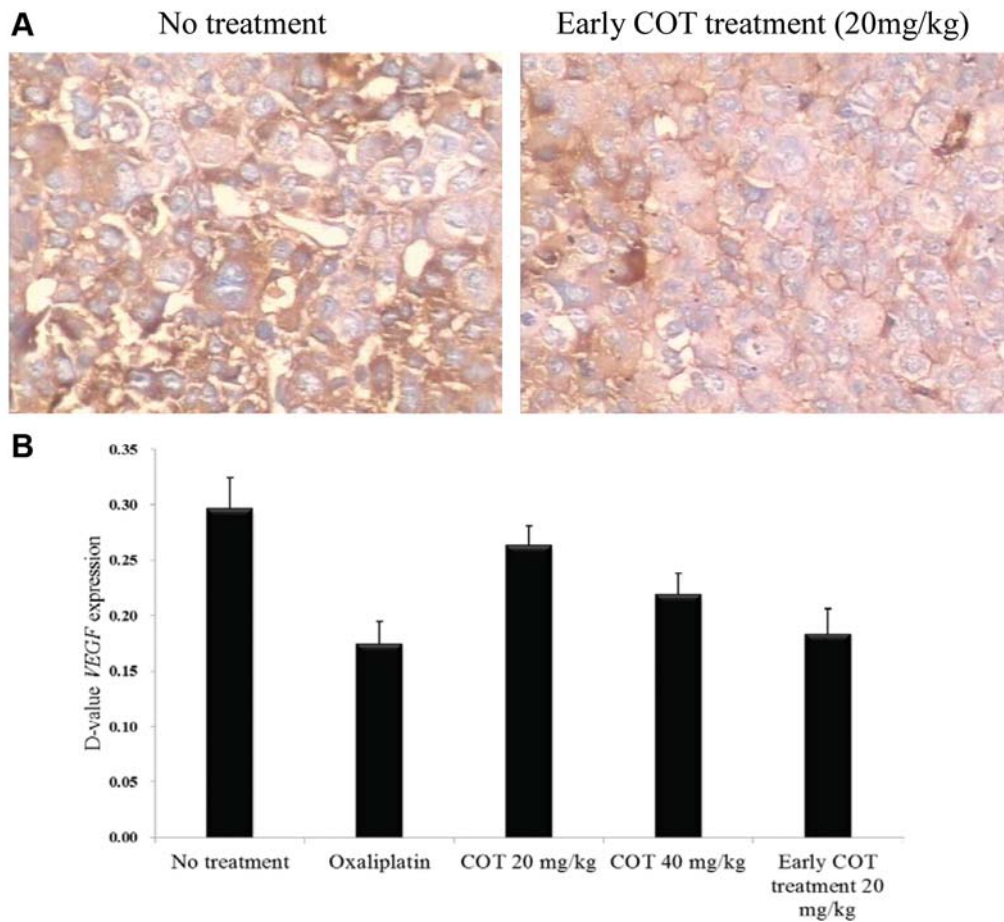


Figure 4. A: Expression of vascular endothelial growth factor (VEGF) protein analyzed by immunohistochemical staining. The brown dots in the cell cytoplasm and membrane indicate expression of VEGF protein in the tumors. B: Dose-related inhibitory efficacy on expression of VEGF protein was found in the tumors from COT- and oxaliplatin-treated mice. D-value of VEGF expression was significantly reduced compared to the control (0.296±0.028) by early COT treatment (0.183±0.023, $p<0.01$), high-dose COT (0.219±0.019, $p<0.01$) and oxaliplatin (0.174±0.021, $p<0.01$) treatments.

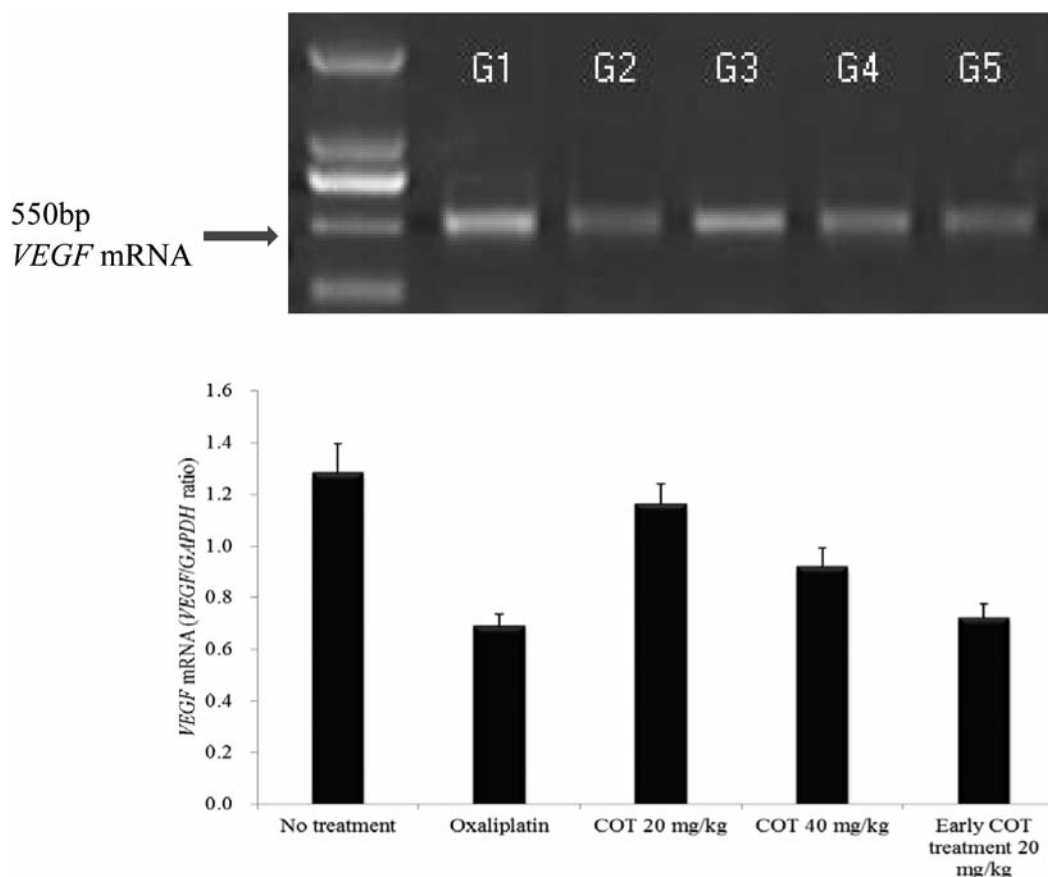


Figure 5. Expression of vascular endothelial growth factor (VEGF) mRNA as analyzed by Reverse Transcription-Polymerase Chain Reaction (RT-PCR). VEGF mRNA expression from the primary tumor was significantly reduced in oxaliplatin (G2, 0.688 ± 0.048 , $p < 0.01$), low-dose *Celastrus orbiculatus* Thunb (COT) (G3, 1.160 ± 0.079 , $p < 0.05$), high-dose COT (G4, 0.918 ± 0.075 , $p < 0.05$) and early COT (G5, 0.720 ± 0.056 , $p < 0.01$) treated mice compared to the control (G1, 1.281 ± 0.114).

differences in metastatic incidence were found between any treatment groups and the control.

Effect of COT and oxaliplatin on tumor VEGF expression.

VEGF protein expression levels of the tumor tissues were analyzed by immunohistochemistry. VEGF protein was found to be expressed in the cytoplasm of all liver cells and the cell membrane of some liver cells. Average optical density (D) of the tumor VEGF expression was significantly reduced by oxaliplatin ($p < 0.05$), low-dose COT ($p < 0.05$), high-dose COT ($p < 0.05$) and early COT treatment ($p < 0.05$) compared to the control group. The tumors from early treatment with COT and oxaliplatin-treated mice had significantly lower VEGF expression levels compared to all other COT-treated mice ($p < 0.01$). The IOD SUM and D values for VEGF expression for each group are presented in Figure 4.

Semiquantitative RT-PCR was used to analyze the expression of VEGF and GAPDH mRNAs in the tumor tissues of all groups. GAPDH mRNA expression as an

internal reference showed no significant difference among the four different treatment groups ($p > 0.05$). As shown in Figure 5, consistent with VEGF protein expression by immunohistochemistry, the tumor VEGF mRNA expression was significantly reduced by oxaliplatin ($p < 0.05$), low-dose COT ($p < 0.05$), high-dose COT ($p < 0.05$) and early COT treatments ($p < 0.05$) compared to the control. VEGF mRNA levels in early COT treated and oxaliplatin-treated mice were significantly lower than in tumor from all other COT-treated mice ($p < 0.01$).

Body weight and toxicity. Clinical observation and body weight measurement of animals during the study were performed to assess toxicity of COT and oxaliplatin treatments. No physical or behavioral signs that indicated adverse effects due to the treatment were observed in any treatment group. All animals were survived until the end of the study. As shown in Figure 6, a stable body weight in the COT-treated groups compared to the control indicated that

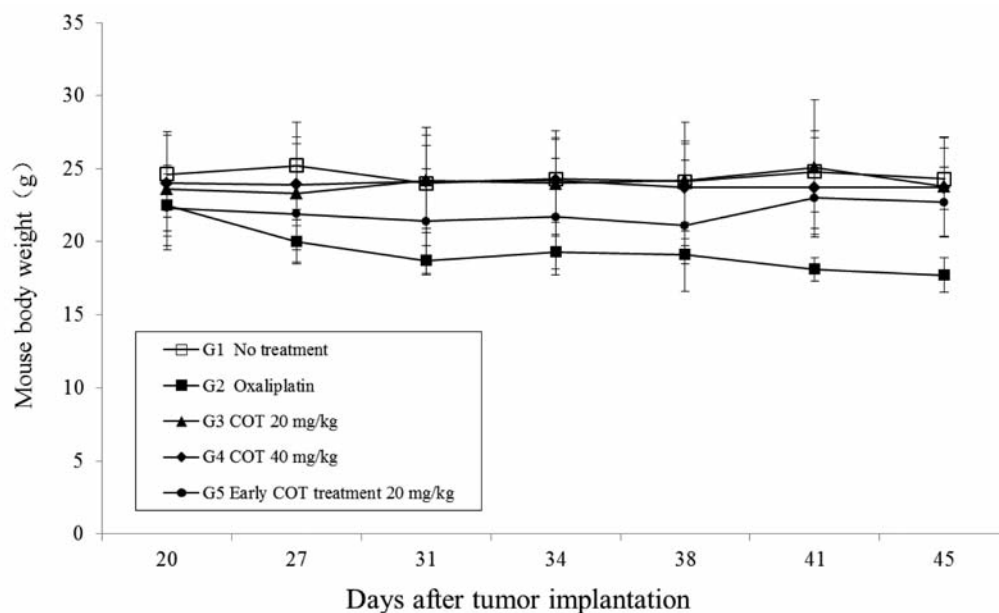


Figure 6. Effect of *Celastrus orbiculatus* Thunb (*COT*) and oxaliplatin on mouse body weight in the orthotopic human Hep-G2- Hep-G2- red fluorescent protein (RFP) hepatocellular carcinoma(HCC) nude mouse model. No significant body weight loss was found in any *COT*-treated mice, oxaliplatin-treated mice exhibited slight body weight loss compared to the control ($p>0.05$).

COT had no obvious toxicity. A slight body weight loss was observed in oxaliplatin-treated mice. However, no significant difference was found compared to the control mice ($p>0.05$).

Discussion

In the present study, we demonstrated that tumor growth in Hep-G2-RFP HCC in the orthotopic nude mouse model was significantly inhibited by early and high-dose (40 mg/kg) *COT* treatment. The antitumor efficacy was found to be dose related. Since platinum-based chemotherapy targets HCC (14), oxaliplatin was selected as the chemotherapeutic agent for comparison in this study. The results of the present study showed that the early treatment with *COT* (20 mg/kg) was the most effective regimen and had similar efficacy to oxaliplatin. Therefore, the present study suggests that *COT* should be used as early treatment for HCC.

To elucidate the mechanism underlying the antitumor efficacy of *COT*, we examined the expression of *VEGF* protein and mRNA of the treated tumors. *COT* and oxaliplatin treatment demonstrated significant efficacy on tumor *VEGF* expression. The results indicate *VEGF* may be a target for *COT*.

In this study we examined the efficacy of *COT* on metastasis in the orthotopic liver tumor mouse model by fluorescence imaging. There were no significant differences in metastatic incidence between mice with *COT* treatments and the control. The reason may due to the relatively low

metastasis frequency of this Hep-G2-RFP HCC mouse model. Further study will be performed to evaluate the efficacy of *COT* on metastasis of HCC using HCC cell lines with higher metastatic potential.

Conclusion

This study demonstrates the inhibitory efficacy of *COT* on the growth of HCC tumor, and *VEGF* inhibition may contribute in part to the inhibition of HCC tumor growth. The results of the present report suggest *COT* has potential to treat HCC.

References

- Huang TK: Modern Compendium of Materia Medica. Beijing: Medical Science and Technology Press of China, Chinese, pp. 1859-1860, 2001.
- Wang M: Research progress of a Chinese herb *Celastrus* on antitumor effect. *J Chinese Medicine* 25(151): 1055-1057, 2010.
- Chang FR, Hayashi K, Chen IH, Liaw CC, Bastow KF, Nakanishi Y, Nozaki H, Cragg GM, Wu YC, Lee KH, Liaw CC, Bastow KF, Nakanishi Y, Nozaki H, Cragg GM, Wu YC and Lee KH: Antitumor agents 228, five new agarofurans, reissantins A2E, and cytotoxic principles from *Reissantia buchananii*. *J Nat Prod* 66(11): 1416-1420, 2003.
- Nagase M, Oto J, Sugiyama S, Yube K, Takaishi Y, Sakato N: Apoptosis induction in HL260 cells and inhibition of topoisomerase by triterpene celastrol. *Biosci Biotechnol Biochem* 67(9): 1883-1887, 2003.

- 5 Qian YY, Zhang H, Hou Y, Yuan L, Li GQ, Guo SY, Tadashi H and Liu YQ: *Celastrus orbiculatus* extract inhibits tumor angiogenesis by targeting vascular endothelial growth factor signaling pathway and shows potent antitumor activity in hepatocarcinomas *in vitro* and *in vivo*. *Chin J Integr Med* 2011 Jul 30. [Epub ahead of print] PMID:21805294.
- 6 Zhang J, Xu YM, Wang WM and Liu YQ. Experimental study on antitumor effect of extract from *Celastrus orbiculatus in vivo*. *China J Chin Materia Medica* 131(18): 1514-1516, 2006.
- 7 Hoffman RM: Orthotopic metastatic mouse models for anticancer drug discovery and evaluation: a bridge to the clinic. *Invest New Drugs* 17(14): 343-359, 1999.
- 8 Rashidi B, An Z, Sun FX, Li XM, Tang ZY, Moossa AR and Hoffman RM: Efficacy of intra-hepatectomy 5-FU on recurrence and metastasis of human hepatocellular carcinoma in nude mice. *Int J Cancer* 91(2): 231-235, 2001.
- 9 Yang M, Baranov E, Wang JW, Jiang P, Wang X, Sun FX, Bouvet M, Moossa AR, Penman S and Hoffman RM: Direct external imaging of nascent cancer, tumor progression, angiogenesis, and metastasis on internal organs in the fluorescent orthotopic model. *Proc Natl Acad Sci USA* 99(6): 3824-3829, 2002.
- 10 Hoffman RM: The multiple uses of fluorescent proteins to visualize cancer *in vivo*. *Nat Rev Cancer* 5(10):796-806, 2005.
- 11 Hoffman RM, and Yang M: Subcellular imaging in the live mouse. *Nature Protoc* 1(2): 775-782, 2006.
- 12 Hoffman RM and Yang M: Color-coded fluorescence imaging of tumor-host interactions. *Nature Protoc* 1(2): 928-935, 2006.
- 13 Hoffman RM and Yang M: Whole-body imaging with fluorescent proteins. *Nature Protoc* 1(3): 1429-1438, 2006.
- 14 Zhu AX, Blaszkowsky LS, Ryan DP, Clark JW, Muzikansky A, Horgan K, Sheehan S, Hale KE, Enzinger PC, Bhargava P and Stuart K: Phase II study of gemcitabine and oxaliplatin in combination with bevacizumab in patients with advanced hepatocellular carcinoma. *J Clin Oncol* 24: 1898-1903, 2006.

Received February 21, 2012

Revised March 15, 2012

Accepted March 16, 2012